

January 06, 2012

Comparison of the kinetic friction of planar neutral and polyelectrolyte polymer brushes using molecular dynamics simulations

Yangpeng Ou
Northeastern University

Jeffrey B. Sokoloff
Northeastern University

Mark J. Stevens
Sandia National Laboratories

Recommended Citation

Ou, Yangpeng; Sokoloff, Jeffrey B.; and Stevens, Mark J., "Comparison of the kinetic friction of planar neutral and polyelectrolyte polymer brushes using molecular dynamics simulations" (2012). *Physics Faculty Publications*. Paper 523. <http://hdl.handle.net/2047/d20004300>

Comparison of the kinetic friction of planar neutral and polyelectrolyte polymer brushes using molecular dynamics simulations

Yangpeng Ou,^{1,*} Jeffrey B. Sokoloff,¹ and Mark J. Stevens²

¹*Physics Department and Center for Interdisciplinary Research in Complex Systems, Northeastern University, Boston, Massachusetts 02115, USA*

²*Center for Integrated Nanotechnologies, Sandia National Laboratories, Albuquerque, New Mexico 87185-1315, USA*

(Received 30 June 2011; revised manuscript received 26 October 2011; published 6 January 2012)

We have simulated the relative shear motion of both neutral and polyelectrolyte end-grafted polymer brushes using molecular dynamics. The flexible neutral polymer brush is treated as a bead-spring model, and the polyelectrolyte brush is treated the same way except that each bead is charged and there are counterions present to neutralize the charge. We investigated the friction coefficient, monomer density, and brush penetration for both polyelectrolyte and neutral brushes with both equal grafting density and equal normal force under good solvent conditions. We found that polyelectrolyte brushes had a smaller friction coefficient and monomer penetration than neutral polymer brushes with the identical grafting density and chain length, and the polyelectrolyte brushes supported a much higher normal load than the neutral brushes for the same degree of compression. Charged and neutral brushes with their grafting densities chosen so that they support the same load exhibited approximately the same degree of interpenetration, but the polyelectrolyte brush exhibited a significantly lower friction coefficient. We present evidence that the reason for this is that the extra normal force contribution provided by the counterion osmotic pressure that exists for polyelectrolyte brushes permits them to support the same load as an identical neutral polymer brush of higher grafting density. Because of the resulting lower monomer density for the charged brushes, fewer monomer collisions take place per unit time, resulting in a lower friction coefficient.

DOI: [10.1103/PhysRevE.85.011801](https://doi.org/10.1103/PhysRevE.85.011801)

PACS number(s): 83.80.Rs, 81.40.Pq

I. INTRODUCTION

Polymers attached to surfaces are important in many applications, such as adhesion [1,2], stabilization of colloid dispersions [3], protection from corrosion [4], flotation of minerals [5–7], oil recovery [8], smart materials [9], and wetting and spreading phenomena [10,11]. A polymer brush consists of polymer chains densely grafted to a solid surface, which is immersed in a solvent. The chains stretch from surfaces and repel each other. The balance between elasticity and repulsion of the chains generates conformations and properties completely different from those for isolated chains. The friction coefficients for surfaces coated with polymer brushes can be extremely low [12–16]. Electrostatic interaction involved in polyelectrolyte brushes results in a number of additional physical properties. Mutual repulsion between polymer segments and electrostatic forces between charged monomers and counterions strongly influence the conformation of the polyelectrolyte brush [17,18]. A great deal of theoretical and experimental research has been conducted to investigate the frictional behavior when lateral sliding occurs between two apposing polymer brushes [19–25]. The normal force and shear force for both neutral polymer brushes and polyelectrolyte brushes have been well studied experimentally by the surface force apparatus (SFA). Through the surface force apparatus, Raviv *et al.* also found a very low friction coefficient when sliding one polyelectrolyte brush relative to the other one [26]. Liberelle used the SFA to study weakly charged polymer brushes to investigate changes in the friction due to changes in the salt (NaCl) concentration [27]. Because of the small distance involved and other limitations of the

experimental apparatus, it is difficult to observe what is happening inside the polymer brushes when they slide relative to each other. Molecular dynamics simulations give us insights into what may be occurring inside the brushes. Using the same bead-spring model, we compared the behavior of neutral polymer brushes and polyelectrolyte brushes through molecular dynamics simulation. Unlike neutral polymer brushes, polyelectrolyte polymer brushes possess counterions, which provide a contribution to the osmotic pressure which supports a significant fraction of the load. Consequently, a polyelectrolyte brush of lower grafting density can support the same load as a neutral brush with the same structure which is not charged. We find that the lower density of the polyelectrolyte brush leads to a lower friction coefficient. References [28–30] used the dissipative dynamics method [31,32] to include explicit solvent molecules in their simulations of polymer brushes. We did not include explicit solvent molecules in our simulations, as was done in Refs. [28–30,33], because including electrostatic interactions and counterions in our simulations was already quite time consuming. The reduction of the friction coefficient found by Galuschko *et al.* is not likely to invalidate our conclusion, since this effect should occur for both neutral and charged polymer brushes. In fact, since the effect is more significant for lower grafting densities, for the case of equal normal force, it will likely reduce the friction coefficient of the charged brushes even further. Since we are not explicitly including solvent molecules, the Langevin equation dynamics that we use should be adequate for our simulations. Although by not including explicit solvent, we cannot treat hydrodynamic interactions between monomers, i.e., interactions mediated by the solvent, we do not feel that they will invalidate our conclusions, again because they should occur for both neutral and charged systems.

*ou.y@husky.neu.edu

II. MODEL

To simulate the motion of polymer brushes sliding relative to each other, we applied the standard bead-spring polymer chain model, which has been used previously in molecular dynamics simulations of polymer brushes [19,23,34]. We investigate polymer brushes grafted onto two apposing surfaces with separation distance D . The number of polymer chains was $N_p = 16$. Each chain contained $N = 32$ monomers and was firmly anchored at one end to the wall surfaces at $z = 0$ or $z = D$. The grafting sites form a square lattice with lattice constant $a = 3.5\sigma$ or 2.4σ , where σ is the length parameter in the Lennard-Jones potential. The corresponding grafting densities ρ_g are $0.082/\sigma^2$ or $0.17/\sigma^2$, which are much larger than $N/(\pi R_g^2)$, where R_g is the radius of gyration of an isolated polymer chain. Therefore, we believed our simulated polymer brushes are in the brush regime. For polyelectrolyte brushes, except for the end-grafted beads, each monomer carries a negative charge, and $N \times N_p$ counterions, each with a positive charge equal to the monomer charge, are explicitly added to neutralize the system [23,35]. Periodic boundary conditions are applied only in x and y direction. Figure 1 shows the configurations of the two apposing polymer brushes.

All particles interact via the shifted Lennard-Jones (LJ) potential,

$$V_{\text{LJ}}(r_{ij}) = \begin{cases} 4\epsilon_{ij}(\sigma_{ij}/r_{ij})^{12} - (\sigma_{ij}/r_{ij})^6 + \frac{1}{4}, & r_{ij} < r_c, \\ 0, & r_{ij} > r_c, \end{cases} \quad (1)$$

where r_{ij} is the distance between two particles, which could be two monomers, two counterions, or a monomer and a counterion. The monomers and counterions have the same bead size and mass, and interact through the same LJ potential parameters, i.e., $\sigma_{ij} = \sigma$, and $\epsilon_{ij} = \epsilon_{\text{LJ}}$ for all particle pairs. Instead of including explicit solvent, we mimic a good solvent by setting the cutoff distance to $r_c = 2^{1/6}\sigma$ in order to keep only repulsive interaction. The bonds of polymer chains are modeled using a finitely extensive nonlinear elastic (FENE) potential,

$$V_{\text{FENE}}(r) = \begin{cases} -0.5kR_0^2 \ln(1 - r^2/R_0^2), & r < R_0, \\ \infty, & r > R_0, \end{cases} \quad (2)$$

where the spring constant $k = 30\epsilon_{\text{LJ}}/\sigma^2$ and the maximum extent distance $R_0 = 1.5\sigma$. The choice of such LJ potential and FENE bond potential parameters prevents bond crossings

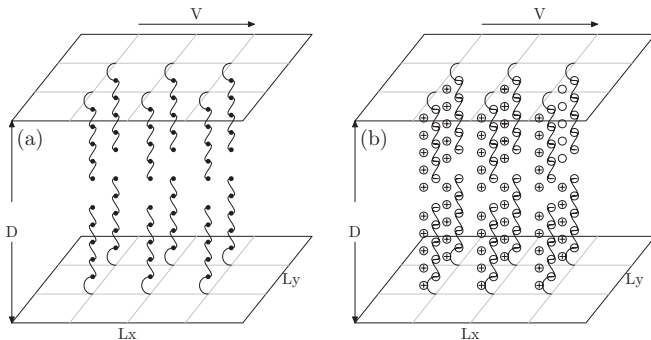


FIG. 1. The schematics of two apposing polymer brushes for (a) neutral brush and (b) charged brush.

and yields realistic dynamics of polymer chains [36,37]. The average bond length, found by minimizing $V_{\text{FENE}}(r) + V_{\text{LJ}}(r)$, is $b = 0.98\sigma$.

For polyelectrolyte brushes, the Coulomb interaction between two charged particles is included. Charged particles interact with each other through a solvent medium, which is presumed to be water in the simulation. Then the Coulomb potential between two charged particles i and j in our simulation system is given,

$$V_{\text{coul}} = k_B T l_B \frac{q_i q_j}{r_{ij}}, \quad (3)$$

where q_i and q_j are charges on two particles in units of an electron charge and l_B is the Bjerrum length, $e^2/4\pi\epsilon\epsilon_0 k_B T$, where ϵ_0 and ϵ are the vacuum permittivity and the dielectric constant of the solvent, respectively. The Bjerrum length of bulk water is 7.1 \AA at room temperature. We choose $l_B = 0.92\sigma$ in our simulation, and therefore σ is 7.75 \AA and the manning ratio $\zeta = l_B/b = 0.94$, where b is the bond length of a polymer chain. The particle-particle particle-mesh (PPPM) method implemented in LAMMPS was used to calculate electrostatic potential between charged particles [38]. All particles except for anchored segments interact repulsively with the walls at $z = 0$ and $z = D$ with the Lennard-Jones (LJ) potential,

$$V_{\text{wall}}(z) = \begin{cases} 4\epsilon(\sigma/z)^{12} - (\sigma/z)^6 + \frac{1}{4}, & z < z_c, \\ 0, & z > z_c, \end{cases} \quad (4)$$

where z is the distance between particle and substrate. The cutoff distance z_c is set to $2^{1/6}\sigma$ to only keep the repulsive interaction. Therefore the total potential energy of the polyelectrolyte brush system is given by

$$V_{\text{total}} = V_{\text{LJ}} + V_{\text{FENE}} + V_{\text{wall}} + V_{\text{coul}}. \quad (5)$$

The simulations are carried out in a constant number of particles (monomers and counterions), constant volume, and constant temperature (NVT) ensemble. Constant temperature is achieved by imposing the Langevin thermostat on all particles except anchored monomers. In this case, the equation of the i th particles except for grating sites is

$$m_i \frac{dv_i(t)}{dt} = -\nabla_i V_{\text{total}} - \gamma m_i v_i(t) + \Gamma_i(t), \quad (6)$$

where $-\nabla_i V_{\text{total}}$ gives net force on particle i by other particles, and γ is the damping constant used to control relaxation rate in order to maintain the desired temperature. $\Gamma_i(t)$ is a random force acting on the i th particle. Those forces satisfy

$$\langle \Gamma_i(t) \Gamma_j(t') \rangle = 6m_i \gamma k_B T \delta_{ij} \delta(t - t'). \quad (7)$$

The motion of particles under the Langevin equation is believed to mimic collisions of monomers with solvent [21]. In our simulations, γ and T are assigned the values $0.5\tau^{-1}$ and $1.2\epsilon_{\text{LJ}}/k_B$, where τ is defined as $\sigma(m/\epsilon_{\text{LJ}})^{1/2}$. In the initial simulations with the two apposing wall surfaces stationary, all three components of the velocity are coupled to the thermal bath. However, in the later simulations with relative movement between two apposing brush substrates, only the v_y (voracity) component is coupled to the reservoir in order to not bias

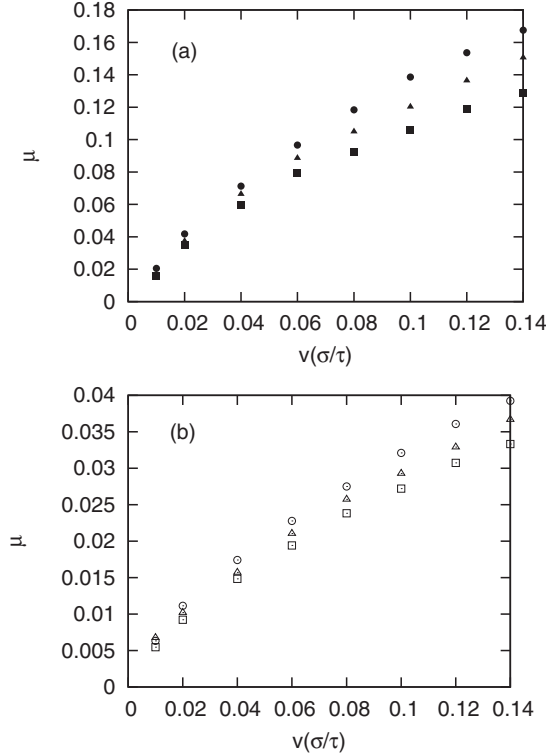


FIG. 2. The variation of friction coefficient as a function of velocity for (a) neutral brushes and (b) charged brushes. The grafting density of polymer brushes, ρ_g , is $0.082/\sigma^2$ for all runs. The solid squares, solid triangles, and solid circles represent results for neutral brushes with $D = 14.0\sigma$, $D = 16.0\sigma$, and $D = 18.0\sigma$, respectively. The dotted squares, dotted triangles, and dotted circles represent results for charged brushes with $D = 14.0\sigma$, $D = 16.0\sigma$, and $D = 18.0\sigma$, respectively. The normal pressures on substrates for these runs are provided in Table I.

the shear flow [19]. The Verlet algorithm is used to integrate Eq. (6) using time step $\delta t = 0.005\tau$.

The simulation in this paper was performed by the following procedure. The initial configuration of the polymer brush was built by randomly placing polymer chains in the simulation box. Counterions were added in the neighborhood of the monomers for polyelectrolyte brushes. To reach stable equilibrium of the polymer brushes, runs with about 1×10^6 time steps, 5000τ in LJ units, are performed on stationary brushes before sliding the top polymer brush relatively to the bottom one. It takes another 3×10^6 time step runs to simulate the movement of polymer brushes during the relative shearing motion described above. We believed the system reached steady shear state after 2.5×10^6 time steps. All results reported in this paper are computed by averaging over the last 5×10^5 time steps.

III. RESULTS AND DISCUSSION

In this section, we presented results of simulations of the relative sliding motions of two brushes. We sheared the system by moving the upper wall at constant velocity $(v, 0, 0)$ while keeping the distance between the two surfaces constant. We calculated the normal force F_n and shear force F_s directly by

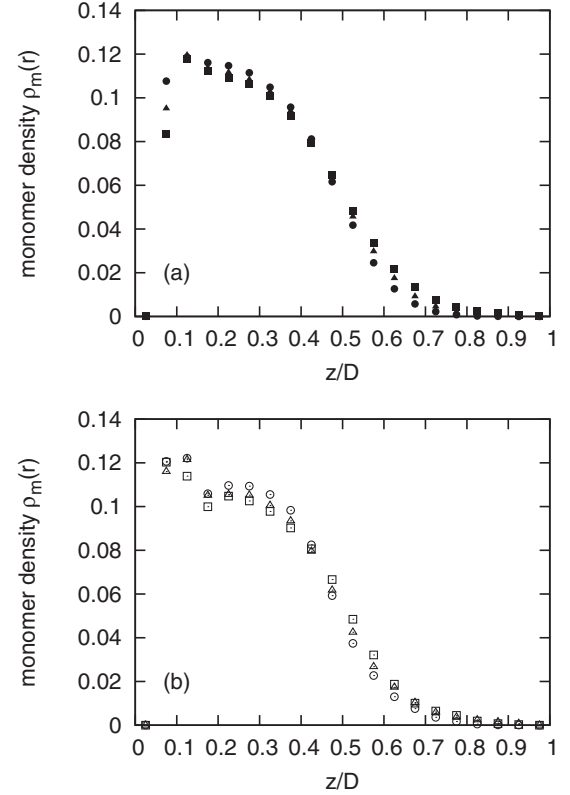


FIG. 3. The monomer density profiles for (a) neutral brushes and (b) charged brushes without the relative sliding. The solid squares, solid triangles, and solid circles represent results for neutral brushes with $D = 14.0\sigma$, $D = 16.0\sigma$, and $D = 18.0\sigma$, respectively; the dotted squares, dotted triangles, and dotted circles represent results for charged brushes with $D = 14.0\sigma$, $D = 16.0\sigma$, and $D = 18.0\sigma$, respectively. For all simulations, the grafting density of polymer brushes, $\rho_g\sigma^2$, is 0.082.

adding together the vertical z components and the horizontal x components, respectively, of forces acting between the substrates and all particles. The corresponding stresses so obtained are labeled σ_n and σ_s , respectively. The friction coefficient is defined as $\mu = \sigma_s/\sigma_n$.

A. Neutral brushes and polyelectrolyte brushes with the same grafting density

In this section, we analyzed the mechanical properties of polymer brushes under shear motion, and compared these properties between neutral and polyelectrolyte brushes with the same grafting density. For both neutral and charged brushes, the polymer chain length N is 32 monomers, the number of polymer chains on each wall N_p is 16, and the spacing between two neighboring chains a is 3.5σ , where σ is the length parameter in the Lennard-Jones potential. The corresponding grafting density is $0.082/\sigma^2$.

Figure 2 shows a comparison of the friction coefficients of the neutral brushes and polyelectrolyte brushes with parameters specified in the figure caption. From our molecular dynamics simulation results, the friction coefficient of a neutral polymer brush is much larger than that of a polyelectrolyte brush with the same grafting density and the same surface

separation distance. The normal force was almost constant for both neutral and charged systems as a function of sliding velocity. However, an increase in the sliding velocity of the top polymer brush results in an increase in the frequency of interactions between the top and bottom brushes' monomers, and an increase in the shear force, which results in an increase of the friction coefficient. When the wall separation distance D was decreased, the normal force and shear force on the wall increased for both neutral and charged brushes. The result comes from stronger interactions between monomers in the system because decreasing the distance between substrates results in an increase in the global monomer density, which can be seen in Fig. 3. Also, the values of normal forces on the walls for the polyelectrolyte brushes are about an order of magnitude greater than the corresponding values for the neutral brushes, even though both of them have the same grafting density and chain length. The difference results from the existence of counterions in the polyelectrolyte brushes, which result in osmotic pressure which adds normal force. Similar results were found in the simulations for neutral brushes by Grest [19].

Figure 4 shows how the monomer density profiles of both neutral and charged brushes respond to different sliding velocities. If bottom and top brushes were to completely repel each other, the bottom and top brushes would occupy space

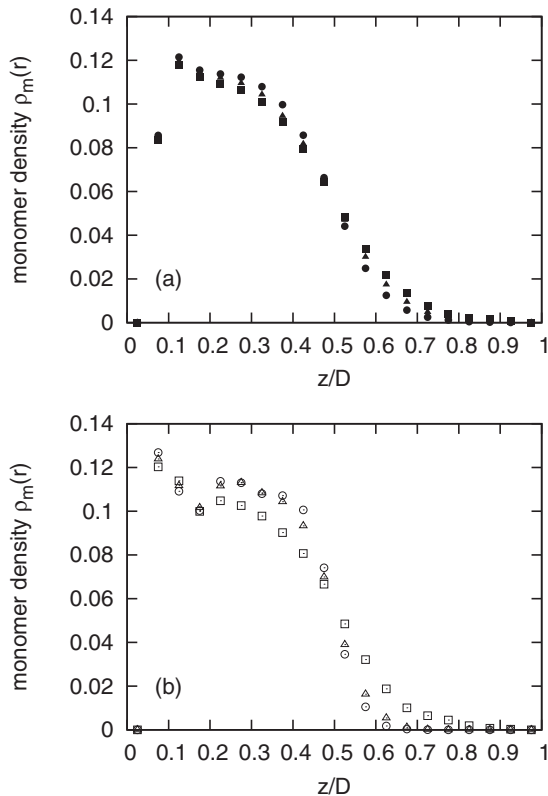


FIG. 4. The monomer density profiles for (a) neutral brushes and (b) charged brushes at the separation distance $D = 14.0\sigma$. The solid squares, solid triangles, and solid circles represent results for neutral brushes with the sliding velocity $v = 0.00\sigma/\tau, 0.04\sigma/\tau$, and $0.10\sigma/\tau$, respectively; the dotted squares, dotted triangles, and dotted circles represent results for charged brushes with the sliding velocity $v = 0.00\sigma/\tau, 0.04\sigma/\tau$, and $0.10\sigma/\tau$, respectively. For all simulation runs, the grafting density $\rho_g\sigma^2$ is 0.082.

$z < D/2$ and $z > D/2$ separately. Therefore, the monomer densities for $z/D > 0.5$ in Fig. 4 represent the fraction of monomers which penetrate into the other brush. The region defined by $z/D > 0.5$ in the monomer density profile quantifies the amount of penetration between top and bottom brushes. For both neutral and polyelectrolyte brushes, the monomer density of the lower brush for $z > D/2$ decreased as the relative sliding velocity between top and bottom brushes increased. The reason is that the increase of relative shear motion between top and bottom brushes increases the interaction frequency between monomers in the brushes. In Figs. 4(a) and 4(b), comparing monomer density profiles at the sliding velocity $v = 0.00\sigma/\tau$ and $0.10\sigma/\tau$ for both neutral and polyelectrolyte brushes, we could see the monomer penetration in the charged polymer brushes decreased with increasing velocity more than for the neutral brushes. Therefore, when the top brush slides relative to the bottom brush, it takes less work to pull these interacting monomers apart for charged brushes.

The amount of interpenetration between the top and bottom brushes when the two wall surfaces are separated by a distance D is defined by [19]

$$I(D) = \frac{\int_{D/2}^D \rho(z) dz}{\int_0^D \rho(z) dz}, \quad (8)$$

where the quantity $\rho(z)$ is the monomer density profile of the lower brush found from Fig. 4. This quantity defines the thickness of the region containing interacting monomers between the top and bottom brushes. The larger the interpenetration between top and bottom brushes, the more interaction between them.

The first result from Fig. 5 is that charged brushes have smaller interpenetration of top and bottom brushes than neutral brushes. Therefore, it takes less work to pull apart these interacting monomers for charged brushes than neutral brushes. The second result from Fig. 5 is that the interpenetration between top and bottom brushes decreases as the relative shear velocity of the top brush increases. The decrease of interpenetration comes about because the monomers interact more frequently for larger velocities.

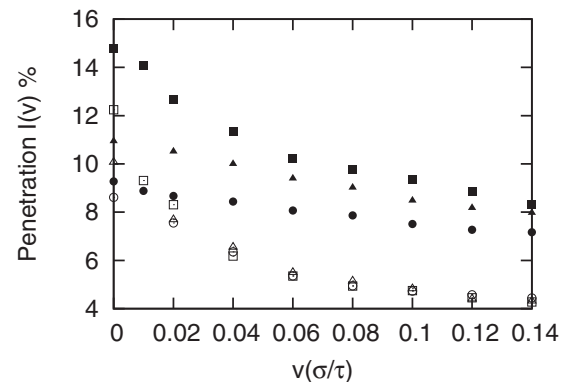


FIG. 5. The variation of interpenetration as a function of velocity for neutral and charged brushes. The labeling system here is the same as in Fig. 2. For both neutral and charged polymer brushes, 16 polymer chains are anchored to the wall surface in a square lattice at the grafting density $\rho_g\sigma^2 = 0.082$.

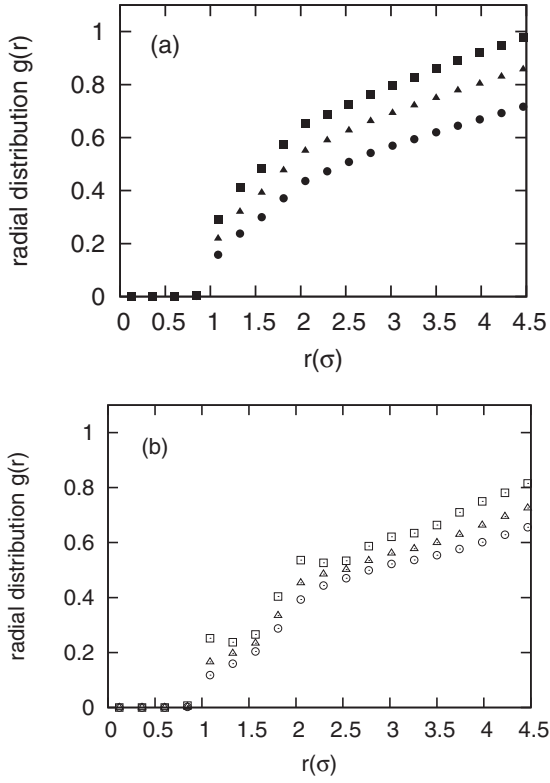


FIG. 6. The radial distribution function between the top brush and bottom brush for (a) neutral brushes and (b) charged brushes with sliding top brushes at constant velocity $v = 0.04\sigma/\tau$. The labeling method here is the same as in Fig. 2. For both neutral and charged polymer brushes, 16 polymer chains are anchored to the wall surface in a square lattice at the grafting density $\rho_g\sigma^2 = 0.082$.

Matsen [39] has performed mean-field theory calculations on two polyelectrolyte brushes in contact. Figure 10 of Ref. [39] gives the degree of interpenetration of the brushes as a function of plate separation. For a plate separation corresponding to $D = 18b$ in our notation, Matsen finds a degree of interpenetration of 0.05 for the highest grafting density that he considers, which is smaller than our grafting density ($0.082/\sigma^2$) for this value of D . Since Matsen's model is for a \ominus solvent (which has no monomer-monomer hard core interaction), however, and our model includes hard core interaction, we do not expect precise agreement, but it is encouraging that the results of the two approaches are not so significantly different.

To determine directly the amount of contact at the interfaces between top and bottom polymer brushes, we present the results of calculations of the radial distribution in Fig. 6. The radial distribution function $g_2(\mathbf{r}_i, \mathbf{r}_j)$ or simply $g(r)$ gives the probability of finding a pair of monomers a distance r apart, relative to the probability expected for a completely random distribution at the same density [40,41]. In the canonical ensemble

$$g(\mathbf{r}_1, \mathbf{r}_2) = \frac{N(N-1)}{\rho^2 Z_{NVT}} \int d\mathbf{r}_3 \dots d\mathbf{r}_N \exp[-\beta \mathcal{V}(\mathbf{r}_1, \dots, \mathbf{r}_N)], \quad (9)$$

where $\mathcal{V}(\mathbf{r}_1, \dots, \mathbf{r}_N)$ is the potential energy of the monomers. The choice $i = 1, j = 2$ is arbitrary in the simulation system

of identical monomers. An equivalent definition takes an ensemble average over pairs

$$g(r) = \rho^{-2} \left\langle \sum_i \sum_{j \neq i} \delta(\mathbf{r}_i) \delta(\mathbf{r}_j - \mathbf{r}) \right\rangle \\ = \frac{V}{N^2} \left\langle \sum_i \sum_{j \neq i} \delta(\mathbf{r} - \mathbf{r}_{ij}) \right\rangle. \quad (10)$$

Here \mathbf{r}_i and \mathbf{r}_j are the position points of monomers in the top and bottom polymer brushes, respectively. It can be thought of as the number of monomer pairs between top and bottom polymer brushes with a given separation r compared to the number of monomer pairs with the same density and separation r in an ideal gas.

From Fig. 6, we can see that the radial distribution function of the neutral brushes is larger than that for the charged brushes close to $r = 1\sigma$, which is about the hard core radius of Lennard-Jones potential in our simulation. The radial distribution close to $r = 1\sigma$ represents the amount of contact between top and bottom polymer brushes. This result is consistent with Fig. 5; both of them show that monomers of neutral brushes have more interactions than monomers of polyelectrolyte brushes when they are compressed together.

In summary, the charged polymer brushes have smaller friction coefficients than identical neutral brushes. From the above analysis, the monomer density profile (Fig. 4), the interpenetration between top and bottom brushes (Fig. 5), and the radial distribution function of two apposing brushes (Fig. 6) show that charged brushes have a smaller number of monomer collisions than neutral brushes, which yields a smaller friction coefficient for charged brushes.

B. Neutral brushes and polyelectrolyte brushes with the same normal force pressure on the walls

In this section, in order to show that a polyelectrolyte brush is a better lubricant than a neutral brush, we compared different behaviors of neutral and polyelectrolyte brushes with the same external pressures exerted on their walls.

Because of the existence of counterions in the polyelectrolyte brushes, the force needed to compress them are many times larger than for neutral brushes with the same grafting density. This difference can be seen in Table I. In order to make the external pressures exerted on substrates of neutral and polyelectrolyte brushes nearly equal, we select different polymer grafting densities for the neutral and charged brushes and keep other parameters, such as the chain length, the same. For example, in Table II, neutral brushes with grafting density

TABLE I. The table gives the normal pressures on wall surfaces with the separation distance D . Both neutral and polyelectrolyte brushes have the same polymer grafting density $\rho_g = 0.082/\sigma^2$.

D (σ)	Neutral brushes $\sigma_n(\epsilon_{LJ}/\sigma^3)$	Polyelectrolyte brushes $\sigma_n(\epsilon_{LJ}/\sigma^3)$
14.0	0.41	6.29
16.0	0.25	3.70
18.0	0.17	2.45

TABLE II. The table gives the normal pressures on wall surfaces for neutral and charged brushes with different grafting densities but the same polymer chain length. Polyelectrolyte brushes are anchored to surface with square lattice constant 3.5σ , which is the same as grafting density $\rho_g = 0.082/\sigma^2$. Neutral brushes are anchored to wall surface with square lattice constant 2.4σ , which is the same as grafting density $\rho_g = 0.174/\sigma^2$.

$D(\sigma)$	Neutral brushes $\sigma_n(\epsilon_{LJ}/\sigma^3)$	Polyelectrolyte brushes $\sigma_n(\epsilon_{LJ}/\sigma^3)$
14.0	5.76	6.29
16.0	3.38	3.70
18.0	2.03	2.45

$\rho_g = 0.174/\sigma^2$ and charged brushes with grafting density $\rho_g = 0.082/\sigma^2$ have close values of normal force pressures on their wall surfaces under different surface separation distances if they have the same chain length.

Figure 7 presents the friction coefficients of neutral brushes with the grafting density $\rho_g = 0.174/\sigma^2$. Compared to the friction coefficients of charged brushes with grafting density $\rho_g = 0.082/\sigma^2$ in Fig. 2, the polyelectrolyte brushes still exhibit lower friction by a factor of about 2. In the previous section, we found that the charged brushes have much lower friction coefficients, and the explanation was that there was more interpenetration of brushes for neutral than polyelectrolyte ones. Figure 8 shows that neutral brushes and charged brushes, with specified grafting densities, have almost the same monomer interpenetration, even under the same external normal pressures on their walls. The surprising fact that they have lower friction coefficients can be explained through a comparison of the radial distribution functions of these two kinds of polymer brushes. The radial distribution function $g(r)$ of neutral brushes with grafting density $\rho_g = 0.174/\sigma^2$ in Fig. 9 has higher values close to $r = 1\sigma$ than charged brushes with grafting density $\rho_g = 0.082/\sigma^2$ in Fig. 6(b). Here, $r = 1\sigma$ is the hard core radius of Lennard-Jones potential in our simulation. Therefore, the larger values of $g(r)$ close to

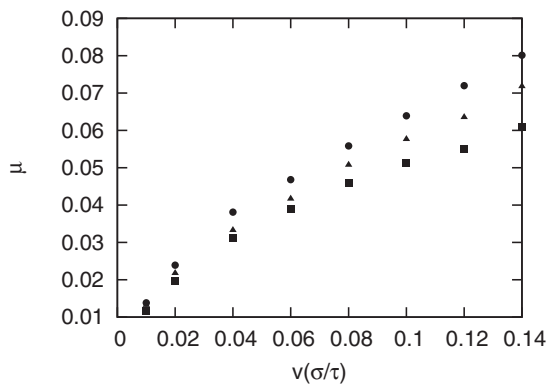


FIG. 7. The variation of friction coefficient as a function of velocity for neutral brushes with grafting density $\rho_g = 0.174/\sigma^2$. The solid squares, solid triangles, and solid circles represent runs for neutral brushes with $D = 14.0\sigma$, $D = 16.0\sigma$, and $D = 18.0\sigma$, respectively. The normal pressures on walls for these runs are provided in Table II.

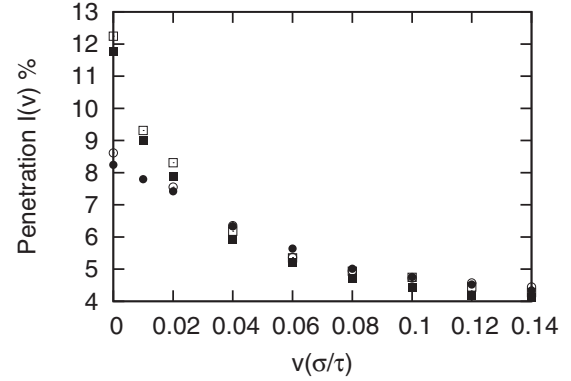


FIG. 8. The variation of the interpenetration as a function of velocity for neutral and charged brushes with almost the same normal force on wall surfaces. The solid squares and solid circles represent results for neutral brushes with $D = 14.0\sigma$ and $D = 18.0\sigma$ at grafting density $\rho_g = 0.082/\sigma^2$; the dotted squares and dotted circles represent results for charged brushes with $D = 14.0\sigma$ and $D = 18.0\sigma$ at grafting density $\rho_g = 0.174/\sigma^2$. For both neutral and charged polymer brushes, 16 polymer chains are anchored to the wall surface in a square lattice.

$r = 1\sigma$ imply more contacts between top and bottom brushes. When the same normal pressure was exerted on substrates of both neutral and polyelectrolyte brushes, the monomer density in the neutral brush would be much larger than the polyelectrolyte brush, and it is reasonable that there would be more interaction, and hence more friction, between neutral brushes than charged brushes.

In summary, for neutral and charged brushes with different grafting densities but the same normal pressures on their wall surfaces, the charged brushes exhibit lower friction than corresponding neutral brushes. The larger friction of the neutral brush results from the larger number of collisions between top and bottom brush monomers.

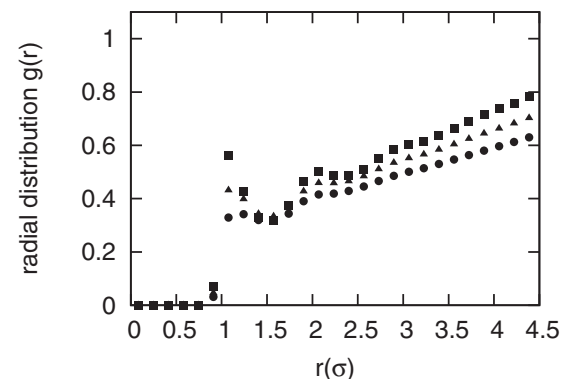


FIG. 9. The radial distribution function $g(r)$ between the top brush and bottom brush for neutral brushes with top brush sliding constant velocity $v = 0.04\sigma/\tau$. The solid squares, solid triangles, and solid circles represent results for neutral brushes with $D = 14.0\sigma$, $D = 16.0\sigma$, and $D = 18.0\sigma$, respectively. For all runs, 16 polymer chains are anchored to the wall surface with the grafting density $\rho_g = 0.174/\sigma^2$.

IV. CONCLUSION

Through applying the standard bead-spring polymer chain model with implicit solvents, we simulated the resulting motion of neutral and polyelectrolyte brushes when they slide relative to each other. Section III A discussed simulation results for neutral and polyelectrolyte brushes with the same grafting density. The counterions in the polyelectrolyte brush provide additional support for external loads, and the polyelectrolyte brush also has smaller interaction between interfaces of the top and bottom brush. Both of these reasons explain why our simulation results demonstrate that neutral brushes have a lower friction coefficient and a lower monomer penetration than a polyelectrolyte brush with the same grafting density. Section III B discussed simulation results for neutral and polyelectrolyte brushes with difference grafting density but the same compression pressure externally exerted on their substrates. Although these two kinds of polymer brush had almost the same monomer penetration, the comparison of

the radial distribution functions between them showed that neutral brushes had much stronger interactions between the top and bottom brushes' interface. That difference probably explained why neutral brushes had a larger friction coefficient than polyelectrolyte brushes even when they are compressed with the same external pressure.

Note added in proof. Recently, we became aware of simulations by Russano *et al.* [42] on friction between bottle brush coated surfaces.

ACKNOWLEDGMENTS

Sandia is a multiprogram laboratory operated by Sandia Corporation, a Lockheed Martin Company, for the United States Department of Energy under Contract No. DE-AC04-94AL85000. This work was performed at the US Department of Energy, Center for Integrated Nanotechnologies, at Los Alamos National Laboratory (Contract No. DE-AC52-06NA25396) and Sandia National Laboratories.

-
- [1] M. Deruelle, L. Leger, and M. Tirrell, *Macromolecules* **28**, 7419 (1995).
- [2] C. Ligoure, *Macromolecules* **29**, 5459 (1996).
- [3] A. Gast and L. Leibler, *Macromolecules* **19**, 686 (1986).
- [4] I. A. Wootton, L. K. Spainhour, and N. Yazdani, *Journal of Composites for Construction* **7**, 339 (2003).
- [5] R. J. and Pugh, *Int. J. Miner. Process.* **25**, 131 (1989).
- [6] E. Bogusz, S. Brienne, I. Butler, S. Rao, and J. Finch, *Minerals Engineering* **10**, 441 (1997).
- [7] A. Boulton, D. Fornasiero, and J. Ralston, *Int. J. Miner. Process.* **61**, 13 (2001).
- [8] J. F. Stanislav, *Rheol. Acta* **565**, 564 (1982).
- [9] I. Roy and M. N. Gupta, *Chemistry & Biology* **10**, 1161 (2003).
- [10] R. C. Advincula, W. J. Brittain, K. C. Caster, and J. R uhe, *Polymer Brushes: Synthesis, Characterization, Applications* (Wiley-VCH, Weinheim, Germany, 2004).
- [11] M. M uller, C. Pastorino, T. Kreer, K. Binder, and L. MacDowell, in ACS Abstracts 231, 416-PMSE (2006).
- [12] J. Klein and E. Kumacheva, *J. Chem. Phys.* **108**, 6996 (1998).
- [13] E. Kumacheva and J. Klein, *J. Chem. Phys.* **108**, 7010 (1998).
- [14] J. Klein, E. Kumacheva, D. Mahalu, D. Perahia, and L. Fetters, *Nature (London)* **370**, 634 (1994).
- [15] H. J. Taunton, C. Toprakcioglu, L. J. Fetters, and J. Klein, *Macromolecules* **23**, 571 (1990).
- [16] J. Klein, *Annu. Rev. Mater. Sci.* **26**, 581 (1996).
- [17] M. Ballauff and O. Borisov, *Curr. Opin. Colloid Interface Sci.* **11**, 316 (2006).
- [18] J. R uhe *et al.*, in *Polyelectrolytes with Defined Molecular Architecture I*, Advances in Polymer Science, Vol. 165 (Springer, Berlin, 2004), pp. 189–198.
- [19] G. S. Grest, *Phys. Rev. Lett.* **76**, 4979 (1996).
- [20] M. Murat and G. S. Grest, *Phys. Rev. Lett.* **63**, 1074 (1989).
- [21] T. Kreer, M. H. M user, K. Binder, and J. Klein, *Langmuir* **17**, 7804 (2001).
- [22] D. J. Sandberg, J.-M. Y. Carrillo, and A. V. Dobrynin, *Langmuir* **23**, 12716 (2007).
- [23] O. J. Hehmeyer and M. J. Stevens, *J. Chem. Phys.* **122**, 134909 (2005).
- [24] Q. Cao, C. Zuo, L. Li, and H. He, *Modell. Simul. Mater. Sci. Eng.* **18**, 075001 (2010).
- [25] J. B. Sokoloff, *J. Chem. Phys.* **129**, 014901 (2008).
- [26] U. Raviv and J. Klein, *Science* **297**, 1540 (2002).
- [27] B. Liberelle and S. Giasson, *Langmuir* **24**, 1550 (2008).
- [28] A. Galuschko, L. Spirin, T. Kreer, A. Johner, C. Pastorino, J. Wittmer, and J. Baschnagel, *Langmuir* **26**, 6418 (2010).
- [29] F. Goujon, P. Malfreyt, and D. Tildesley, *Chem. Phys. Chem.* **5**, 457 (2004).
- [30] P. Malfreyt and D. J. Tildesley, *Langmuir* **16**, 4732 (2000).
- [31] P. Hoogerbrugge and J. Koelman, *Europhys. Lett.* **19**, 155 (1992).
- [32] P. Espanol and P. Warren, *Europhys. Lett.* **30**, 191 (1995).
- [33] F. Goujon, P. Malfreyt, and D. J. Tildesley, *Mol. Phys.* **103**, 2675 (2005).
- [34] M. Murat and G. Grest, *Macromolecules* **22**, 4054 (1989).
- [35] C. Seidel, *Macromolecules* **36**, 2536 (2003).
- [36] K. Kremer and G. Grest, *J. Chem. Phys.* **92**, 5057 (1990).
- [37] P. A. Thompson, G. S. Grest, and M. O. Robbins, *Phys. Rev. Lett.* **68**, 3448 (1992).
- [38] E. L. Pollock and J. Glosli, *Comput. Phys. Commun.* **95**, 93 (1996).
- [39] M. Matsen, *Eur. Phys. J. E* **34**, 1 (2011).
- [40] J. P. Hansen and I. R. McDonald, *Theory of Simple Liquids*, 2nd ed. (Academic Press, New York, 1986).
- [41] M. P. Allen and D. J. Tildesley, *Computer Simulation of Liquids* (Clarendon Press, New York, 1989).
- [42] D. Russano, J.-M. Y. Carrillo, and A. V. Dobrynin, *Langmuir* **27**, 11044 (2011).